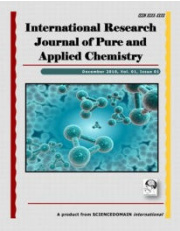

International Research Journal of Pure & Applied Chemistry
2(2): 130-143, 2012

SCIENCEDOMAIN *international*
www.sciencedomain.org

Effect of Zirconium Substitution on the Electrical Properties of Ferroelectric $(Bi_{0.5}Na_{0.5})_{0.94}Ba_{0.06}TiO_3$ Ceramics

Enyew Amare Zereffa[1*] and Alamanda Vara Prasadarao[1]

[1]Department of Inorganic and Analytical Chemistry, School of Chemistry, Andhra University, Visakhapatnam, India.

Authors' contributions

This work was carried out in collaboration with all authors. AVP proposed the study and supervised the work. EAZ performed the experimental work and analysis, wrote the first draft and managed literature searches. Both the authors read and approved the final manuscript.

Research Article

Received 22nd April 2012
Accepted 9th June 2012
Online Ready 16th June 2012

ABSTRACT

Ceramic samples of Zirconium substituted Bismuth Sodium Barium Titanate of composition $(Bi_{0.5}Na_{0.5})_{0.94}Ba_{0.06}(Ti_{1-x}Zr_x)O_3$ with x = 0.0,0.04,0.08,0.1 and 0.2 have been synthesized following solid-state method. X-ray diffraction studies indicated the formation of phase pure materials with rhombohedral structure for $0.0<x<0.1$. A small extra peak near 2θ ~ 28' is noticed for composition x = 0.10. SEM studies indicated substitution of Zr led to an increase in grain size. Dielectric studies revealed a decrease in dielectric constant with Zr substitution up to x = 0.08. Sample with x = 0.10 showed paraelectric behavior indicating the critical concentration of Zr necessary for ferroelectric and paraelectric behavior in those samples lies between 0.08 and 0.10. Impedance measurements showed grain boundary effect and negative temperature coefficient of resistivity behavior. A.C and D.C activation energies have been computed using Arrhenius relation from subsequent temperature regions for two different frequencies of 1 KHz and 10 KHz.

**Corresponding author: enyewama@yahoo.com;*

Keywords: $(Bi_{0.5}Na_{0.5})_{0.94}Ba_{0.06}TiO_3$; dielectric properties; ferroelectric properties; sintering; microstructure.

1. INTRODUCTION

Perovskite type mixed oxides such as $PbTiO_3$, $Pb(Zr,Ti)O_3$, $Pb(Mg_{1/3}Nb_{2/3})O_3$ etc have been found to be extensively useful because of their excellent ferroelectric properties. However, in order to minimize the use of toxic lead, several other materials have been investigated, of which bismuth sodium titanate (BNT) was found to be promising as an environmentally friendly alternative to PZT (Smolenskii et al., 1961). (Sakata and Masuda, 1974) reported that BNT ceramics exhibit a large remnant polarization, P_r= 38cm^2, a high Curie temperature (T_c=320℃) and a very interesting anomaly of a low temperature ferroelectric to antiferroelectric transition at 200℃. Nevertheless, because of its high coercive field, E_c= 73KV/cm and relatively large conductivity, pure BNT is difficult to be poled, which can be overcome by forming solid solutions with $BaTiO_3$ (Takenaka et al., 1991), $PbTiO_3$ (Kuharuangrong and Schulze, 1996), $NaNbO_3$ (Takenaka et al., 1997), Bi_2O_3-Sc_2O_3 (Nagata and Takenaka, 1997), La_2O_3 (Herabut and Safari, 1997), $BiFeO_3$ (Nakada et al., 1999), $KNbO_3$ (Lu et al., 2007), $Bi_{0.5}K_{0.5}TiO_3$ (Thongtha and Bongkarn, 2011), etc. Among these systems, bismuth sodium barium titanate $(Bi_{0.5}Na_{0.5})_{1-y}Ba_yTiO_3$ (BNBT) with y=0.06 is reported to show morphotropic phase boundary with enhanced piezoelectric performance of k_{33}=0.55, k_{31}=0.19, d_{33}=125pC/N. The piezoelectric properties of BNBT were further modified by doping with cations like La^{+3} (Li et al., 2003), Mn^{+2} (Fan et al., 2007), Ag^{+} (Wu et al., 2007), Co^{+3} (Xu et al., 2008), Ce^{4+} (Shi and Yang, 2009), Nb^{+5} (Wang et al., 2010) etc. Our extensive literature survey indicated that no attempt has been made so far to characterize the electrical properties of Zirconium substituted $(Bi_{0.5}Na_{0.5})_{0.94}Ba_{0.06}(Ti_{1-x}Zr_x)O_3$ (BNBTZ) ceramics using dielectric spectroscopy technique. The present paper describes the synthesis, structure, dielectric (ε), impedance (Z*), thermal and conductivity (σ) of BNBTZx in the studies range of 0≤x≤0.2.

2. EXPERIMENTAL DETAILS

2.1 Sample Preparation

Samples of $(Bi_{0.5}Na_{0.5})_{0.94}Ba_{0.06}$ $Ti_{1-x}Zr_x)O_3$ (BNBTZx) ceramics with x=0.0, 0.04, 0.08, 0.10 and 0.20 have been prepared by solid state method. The starting materials are Bi_2O_3 (99.999%, High Media), Na_2CO_3 (99.5%, Sigma Aldrich.), $BaCO_3$ (99.9%, Wako Pure Chemical Industries Ltd.), TiO_2 (99.9%, Sigma Aldrich) and ZrO_2 (99.9% Sigma Aldrich). Weighed powders as per stoichiometry were mixed well in dry and methanol medium in an agate mortar. An extra amount of 3 wt% Bi_2O_3 and Na_2CO_3 were added to the initial mixture to compensate for the respective losses of bismuth and sodium at high temperature. The resulting well ground mixture was calcined at 850℃ for 2 hrs. Phase purity of the final product was investigated by x-ray diffraction (XRD). The calcined powder was mixed with water solution of polyvinyl alcohol (3 wt %) as binder and then pelletized. The pellets were placed on a platinum foil and covered by platinum crucible to minimize evaporation of bismuth and sintered at 1150℃ for 2hrs in a programmable furnace at 5℃ per minute heating and cooling rate with an intermediate shocking time 1hr at 500℃ for burning of organic binder. Silver paste was coated on both sides of the polished surface of the pellet and the coated pellets were curried at 600℃ for 1 hr.

2.2. Characterization Techniques

Phase purity of the final calcined powders was investigated with x-ray diffractometer (PANalytical- X' Pert PRO, Japan) at room temperature, using Nickel filter Cu-K_α radiation (λ = 1.54059 Å), over a wide range of $10° \leq 2\theta \leq 80°$ with a scanning speed of $2° \text{ min}^{-1}$. Microstructural investigations of the sintered ceramic samples were performed on the fractured surface of the sample using SEM (JEOL-JSM-6610LV, Tokyo, Japan). Energy Dispersive X-ray Spectroscopy (EDS) was used to detect x-rays emitted from the sample during bombardment with an electron beam to identify the elemental composition of the analyzed volume.

2.3 Dielectric Measurements

Measurements of capacitance (C), loss tangent (tanδ), complex impedance(z*), resistance (R) and phase angle (Φ) up to 400℃ in the frequency range of 100 Hz - 1 MHz were measured in parallel and series with phase sensitive multi meter (N4L PSM 1700) Japan, with heating rate of 3℃/min.

2.4 Thermal Analysis

Differential scanning calorimeter (DSC) is used to study phase transitions temperature of the ceramic samples. The experiments were conducted on powder samples in air atmosphere at a flow rate of 40ml/min with a heating rate of 3℃/min in the temperature range of 30-600℃ using (METTLER TOLEDO, DSC 823e, Japan) calorimeter.

3. RESULTS AND DISCUSSION

3.1. X-Ray Diffraction

Fig. 1 shows the XRD patterns of pure and zirconium substituted BNBTZx powders for x=0.0, 0.04, 0.08, 0.10 and 0.20. It is evident that the rhombohderal phase (indicated by the peaks at 22.7, 32.4, 46.4, 57.7 and 67.67°) has been already formed after calcination at temperature of 850℃ for 2hrs, but there is a small extra peak near to $2\theta \sim 28°$ for BNBTZ10 and additional one more extra peak around $2\theta \sim 32°$ for the higher Zr dopant BNBTZ20. At higher calcination temperature about 950℃, these extra peaks still remained in the XRD pattern. All the XRD patterns of BNBTZX compositions for $0 \leq x < 0.1$ are in good agreement with that of rhombohedral $Bi_{0.5}Na_{0.5}TiO_3$ (JCPDS file number 36-0340) and the presence of extra peaks at $2\theta = 28°$ and 32° in the composition range of $0.1 \leq x \leq 0.2$ are due to the presence of monoclinic ZrO_2 (JCPDS file number: 89-9066), which means the maximum limits for Zr^{4+} to enter the crystal lattice of BNBT is between 0.08 and 0.10. Average particle size and lattice strain of the calcined powders were determined using William Son Hall Technique. Calculated values of lattice parameters, density, average particle size and average lattice strain are given in Table 1.

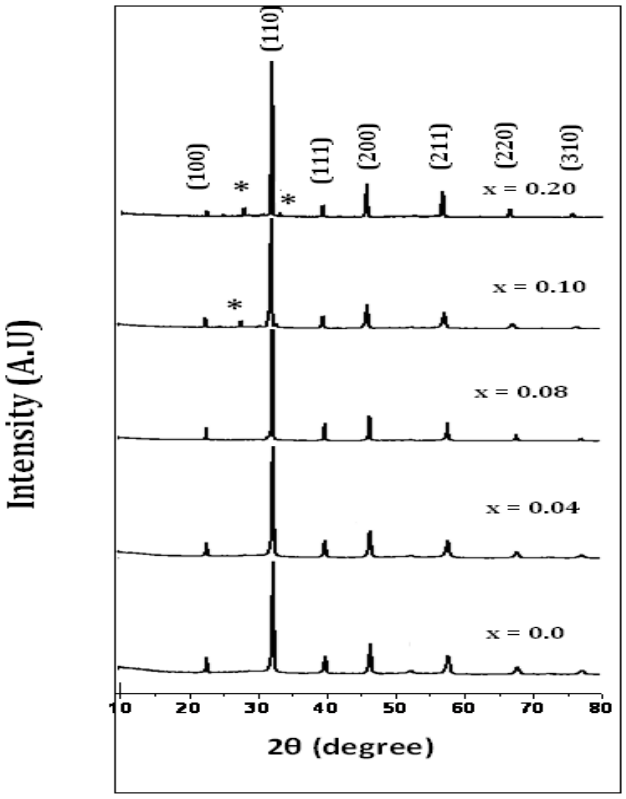

Fig. 1. X-ray diffraction patterns of BNBTZx ceramics for x = 0.0, 0.04, 0.08, 0.1& 0.2

Table 1. Lattice parameters and related properties of BNBTZx

Composition	a(Å)	α (°)	Crystallite size (nm)	Lattice strain ε(x10^{-3})	Experimental density(g/cc)	%Relative density
BNBT	3.899	89.79	44	1.6	5.670	94%
BNBTZ4	3.893	90.03	49	2.2	5.731	95%
BNBTZ8	3.901	90.01	54	2.6	5.632	93%
BNBTZ10	3.933	89.96	78	2.97	5.713	96%

3.2 Scanning Electron Microscopy

Sintered samples were prepared for SEM characterization by coating the fractured surface of pellets sintered at 1150℃ with gold using Auto Fine Coater (JFC-1600 Japan) for 90 seconds. The microstructures of the sintered BNBTZx samples with x = 0.0, 0.04, 0.08 and 0.1 were observed using SEM and micrographs of the samples are shown in Fig. 2a. All these samples are very dense with uniformly distributed grains. A slight change in grain size was observed with addition of Zr^{4+} in the tested range. This may be due to the replacement of small ionic radii Ti^{4+} (r_6^{4+} = 0.62Å) by large ionic radii of Zr (r_6^{4+}=0.72Å) (Suchanicz et al., 2010). The energy dispersive spectrometry (EDS) was used to identify the elements present in the prepared samples by taking a selective portion of SEM image. The spectra of Fig. 2(b & c) shows the elements present in BNBT and BNBTZ4 sintered samples.

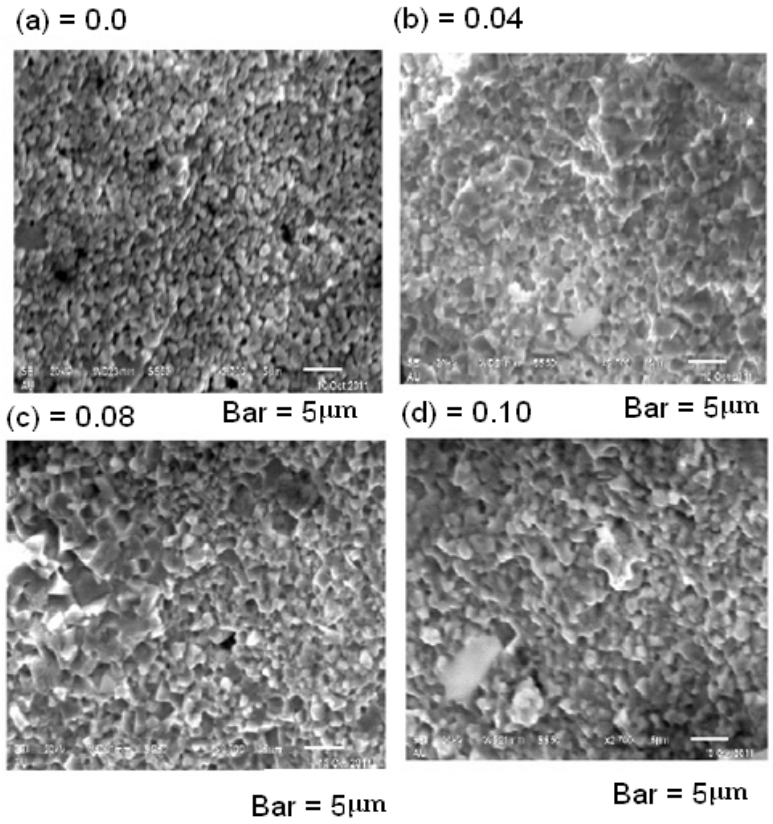

Fig. 2a. SEM micrographs of fractured surface of BNTBZx sintered samples at 1150℃ for 2 hrs for: (a) x = 0.0 (b) x = 0.04, (c) x = 0.08 d) x = 0.10

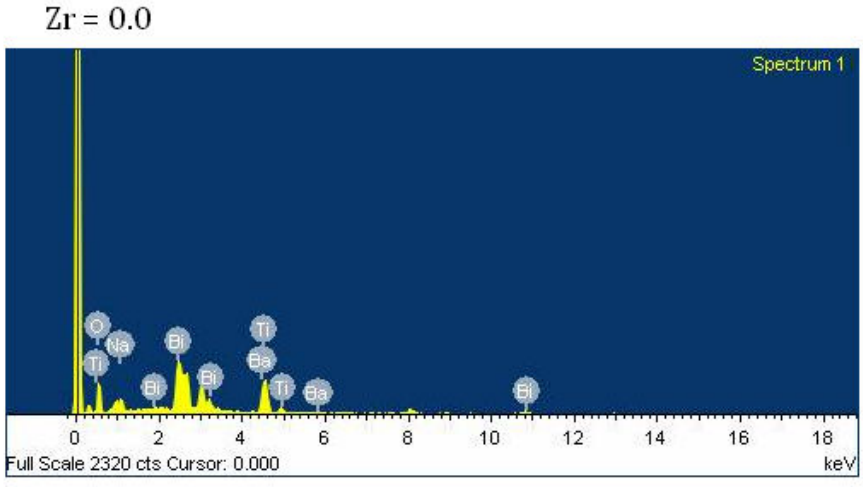

Fig. 2b. EDS spectrum of $(Bi_{0.5}Na_{0.5})_{0.94}Ba_{0.06}Ti_{1-x}Zr_x)O_3$. x = 0.0

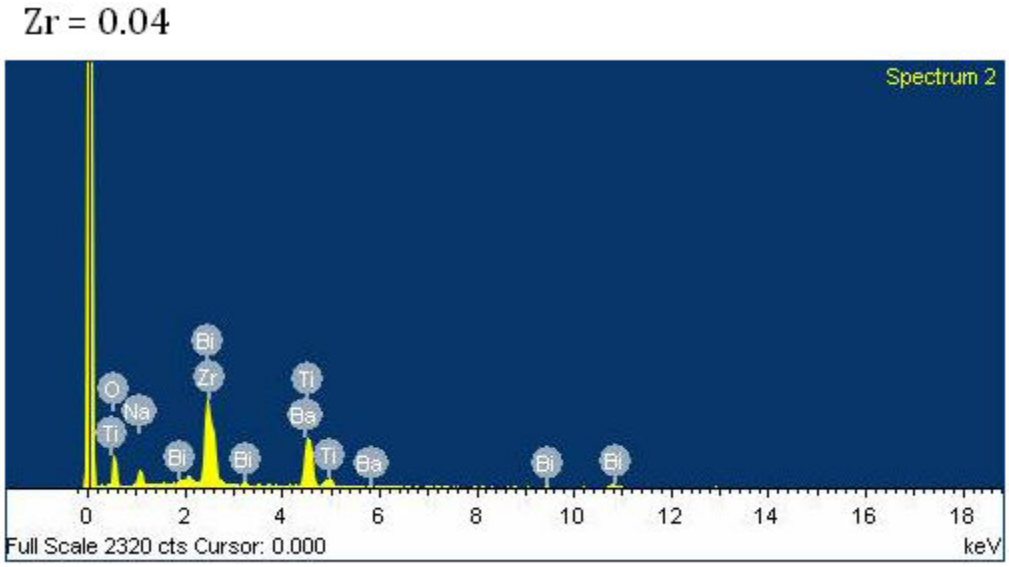

Fig. 2c. EDS spectrum of $(Bi_{0.5}Na_{0.5})_{0.94}Ba_{0.06}Ti_{1-x}Zr_x)O_3$. x = 0.04.

3.3. Dielectric Spectroscopy

Adding dopants to the base BNBT material can modify the dielectric properties in various ways and create a material with a specific desired response. Zirconium was added to BNBT according the formula, $(Bi_{0.5}Na_{0.5})_{0.94}Ba_{0.06}(Ti_{1-x}Zr_x)O_3$, with x ranging from 0.0 to 0.1. As shown in the above formula, zirconium is a B-site dopant. Fig.3 depicts temperature dependence of the real part (ε') of dielectric constant, and dielectric loss (tanδ) of pure and Zr doped BNBT samples at 1, 10, and 50 kHz frequencies respectively. The dielectric constant versus temperature curves in figure 3 exhibit broad peaks with maximum values at T_m (the temperature of permittivity maxima) towards higher values with increasing frequency. This is a clear indication of relaxer behavior of the materials. In normal ferroelectrics the depolarization temperature (T_d) and the maximum temperature (T_m) usually coincide with each other and it is denoted as Curie temperature (T_c). Chu et al., 2002 suggested that the phase transition between ferroelectric phase and paraelectric phase in doped BNT ceramics cannot be expected to occur at a specific temperature due to cation disorder by random distribution of Na^+, $Ba^{2+}$and Bi^{3+} at the *A* sites of the lattice. From Fig. 3 it is clearly seen has the dielectric loss or tanδ goes down to the minimum values in the temperature range of 250-300℃ and then goes up for all frequencies above 300℃ temperature. The anomalous behavior at temperature which coincides with T_m at different frequencies has been observed. This type of tanδ at T_m has been attributed to the reduction in the domain wall contribution to the dielectric loss, (Rao et al., 2007) and the observed dispersive loss at high temperature is probably due to localized ionic conductivity. As it is seen from Fig. 4, the dielectric constant and dielectric loss curves for BNBTZ10 are different from the rest. The curves become flatter and the dielectric constant becomes lowered while their respective dielectric loss increases. Sample with x=0.10 showed paraelectric behavior indicating the critical concentration of Zr necessary for ferroelectric and paraelectric behavior in those samples lies below 0.10. The reason for peak suppression may be due to size difference. Zirconium has a larger ionic radius than titanium and this leads to a decrease in polarizability. As the amount of zirconium increases, the amount of polarization contributed by the titanium ions decreases; therefore,

the relative permittivity also decreases, as seen in the graph. Similar observation has been made by (Lee et al., 2001), in the system (1-x)$Na_{0.5}Bi_{0.5}TiO_3$-x$PbZrO_3$. Fig.5 depicted the Curie and depolarization temperature as function of Zr concentration obtained from differential scanning calorimeters measurements made on powder samples of BNBTZx by (DSC 823e METTLER TOLEDO, Japan) calorimeter to study the influence of zirconium doping on the two anomalous transition temperatures namely ferroelectric to antiferroelectric (FE- AFE) and ferroelectric to paraelectric (FE-PE) up to 600℃ with the heating rate of 3℃/min. Here, the temperature where the transition between ferroelectric phase and anti-ferroelectric phase is called a depolarization temperature (T_d), while the transition temperature between ferroelectric and paraelectric is called Curie temperature (T_c). Both the FE-PE transition and FE-AFE transition temperatures values slightly decrease with increase in Zirconium concentration with references to pure BNBT by (Takenaka et al., 1991; Xu et al., 2008).

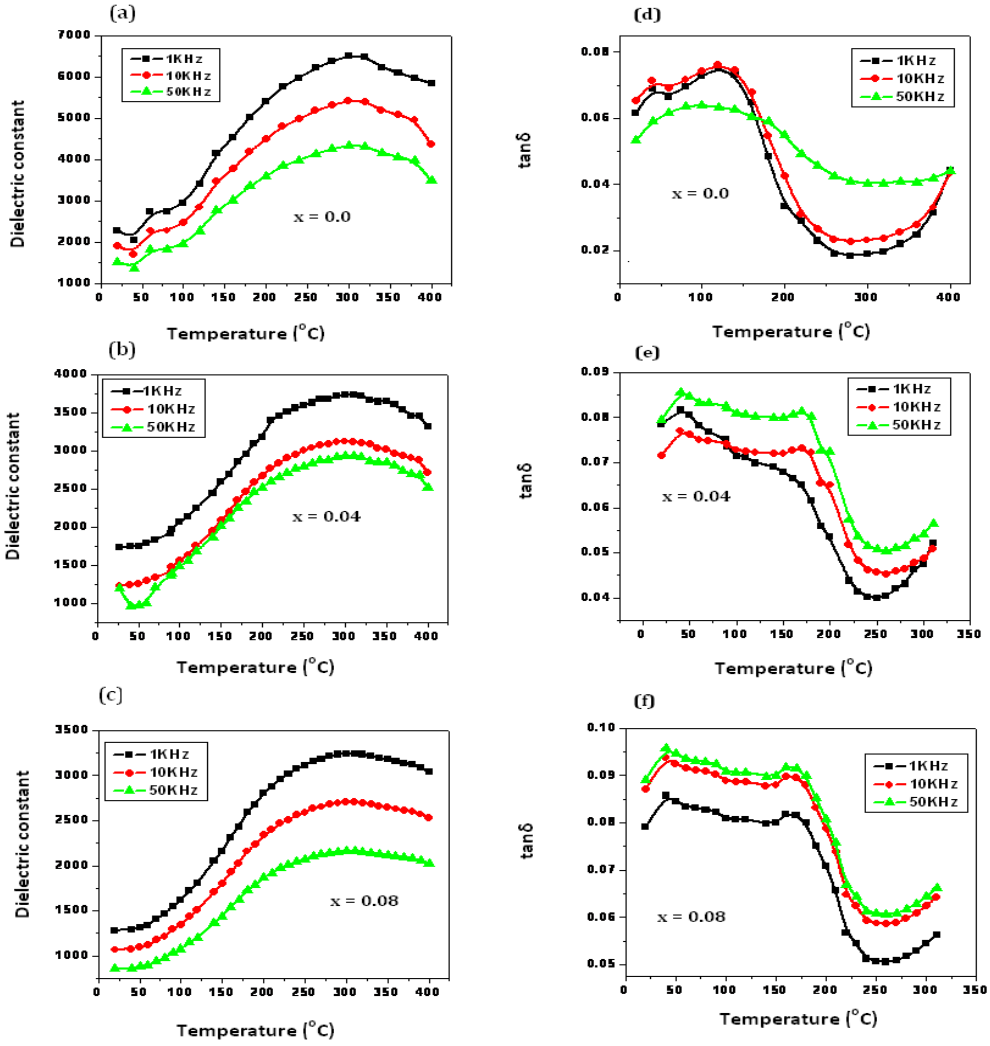

Fig. 3. Variation of dielectric constant Fig. (a-c) and dielectric loss Fig. (d-f) with temperature for BNBTZx ceramic samples (where x = 0.0, 0.04.0.08) at the frequency of 1, 10 and 50 KHz

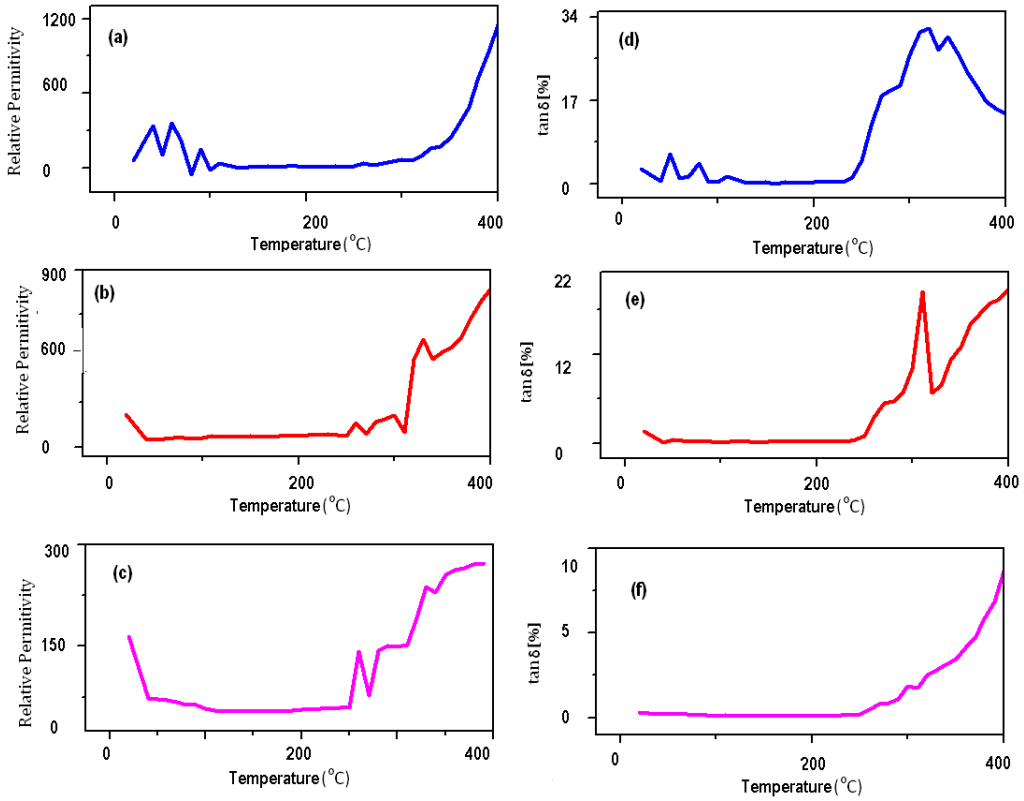

Fig. 4. Variation of dielectric constant [Fig. (a-c)] and dielectric loss [Fig. (d-f)] with temperature for BNBTZ10 ceramic at the frequency of: 1, 10 and 50 KHz.

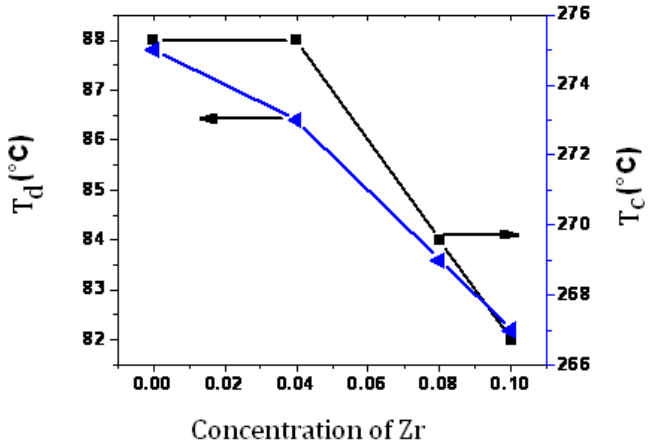

Fig. 5. Depolarization and curie temperatures as a function of Zr concentration

Fig. 6 depicts the frequency dependence of real (ε') and imaginary (ε") dielectric constant at different temperatures for BNBTZ4. It is clear from the figure that ε'(ω) decreases with

increasing frequency. The observed decrease of ε' with frequency is greater at higher temperatures. According to (Srivaslava et al., 1979), the increase of ε' at lower frequencies for polar materials is attributed from the contribution of multi component polarization mechanisms (i.e. electronic, ionic, orientation and space charge). At higher frequency the dipoles cannot rotate rapidly, so that their oscillations lag behind those of the field. As the frequency is further raised the dipole will be completely unable to follow the field and the orientation polarization ceases, so ε' decreases and attain a constant value at high frequencies which is due to the interfacial polarization (Hegab et al., 2007). As depicted in Fig.6b ε" decreases with frequency up to 100 KHz and reach minimum points and then go up to their respective maximum at about 200 KHz for each measurement temperature and again goes down to the minimum point at about 400 KHz and finally start slightly increasing.

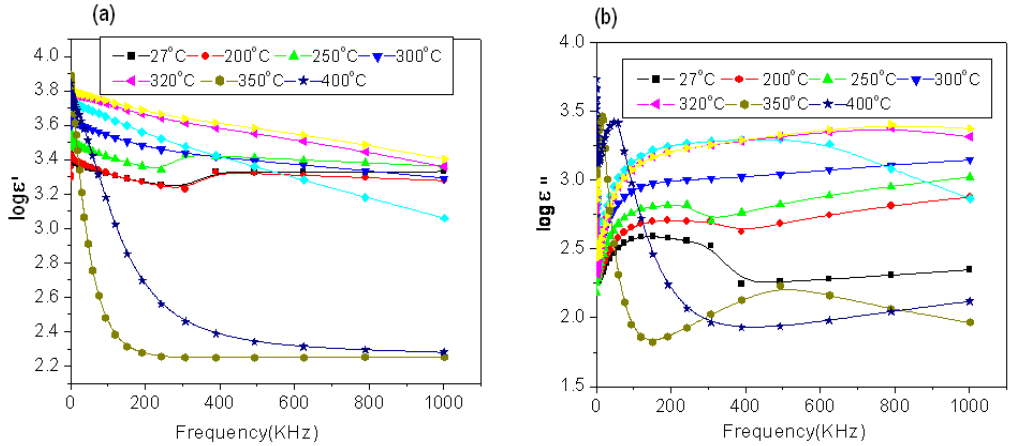

Fig. 6. Frequency dependency of (a) real (ε') and (b) imaginary (ε") dielectric constant at different temperatures for BNBTZ4

3.4. Electrical Conductivity Studies

3.4.1 Impedance plot

Figs. 7(a-d) and their insets show the dependence of the real (*Z'*) and imaginary (*Z"*) parts of impedance on frequency at various temperatures for BNBTZx system. The value of *Z'* decreases with increasing temperature as well as with increasing frequency which shows that the material has negative temperature coefficient of resistance (NTCR). The loss spectra shown in Fig. 7(c-d) are characterized by some important features in the pattern of appearance of a peak (Z''_{max}), asymmetric peak broadening (inset of Fig 7(c-d)) and the decreased of values of *Z"*max which shift to higher temperatures with the increasing frequency. The asymmetric broadening of peaks in frequency in the explicit plots of *Z"* suggests that there is a spread of relaxation times, i.e. the existence of a temperature dependent electrical relaxation phenomenon in the materials.

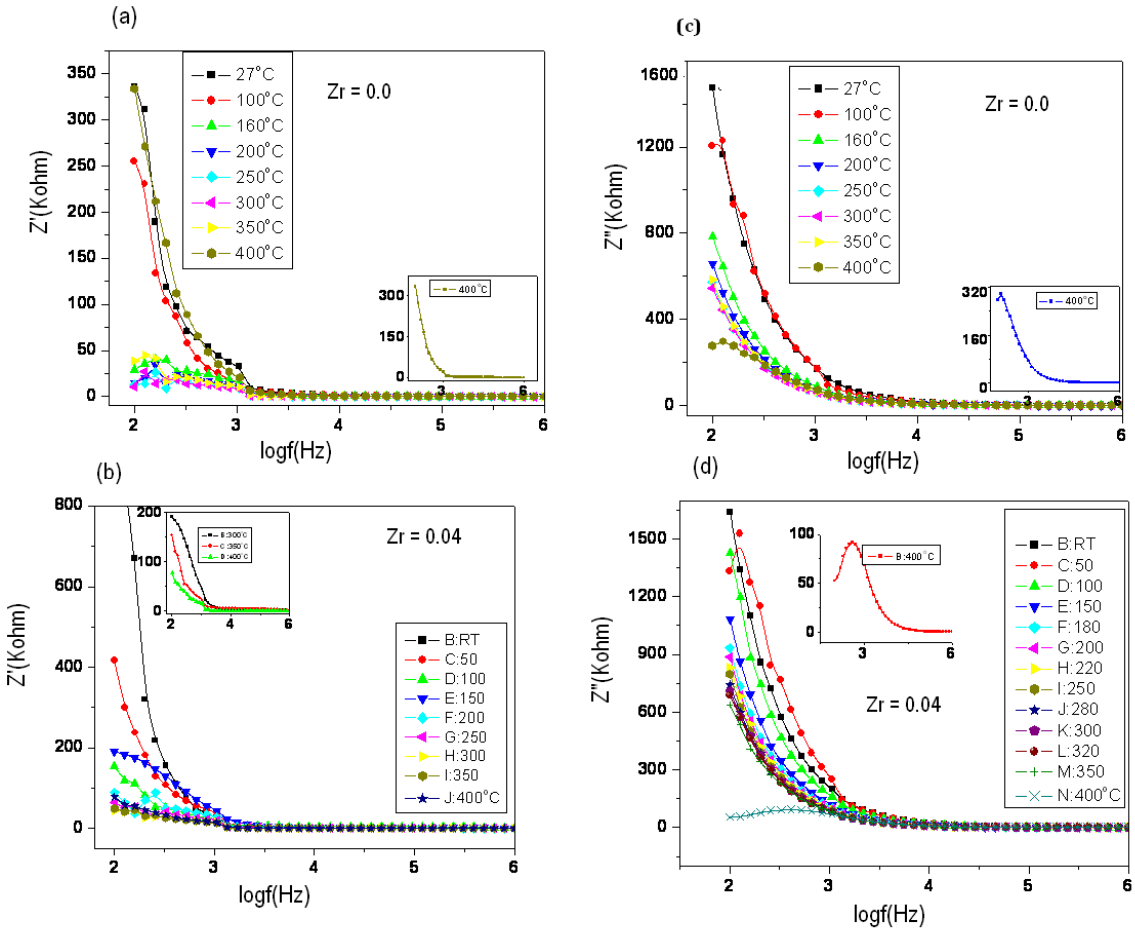

Fig. 7. Frequency dependence of real (7a &b) and imaginary (7c & d) complex impedance of BNBTZx for x = 0.0 & 0.04 ceramic samples at various temperatures. The inset shows an enlarged view at 350℃ and 400℃

Fig. 8 shows the complex impedance plots at various temperatures from which it may be observed that the impedance data at lower temperatures do not take the shape of a semicircle but rather resemble a straight line, suggesting the insulating behavior of ceramic samples. It can also be seen that with the increase in temperature the slope of the lines decreases, and the lines bend towards the real (Z') axis. In the temperature about 300℃ a single semicircle and above 350℃ two semicircles could be obtained with different values of resistance for grain (R_b) and grain boundary (R_{gb}) as depicted on the insets of Fig.8c. This indicates an increase in conductivity of the sample with the increase in temperature. Hence, the grain and grain boundary effects could be separated at these temperatures. It also observed that the peak maxima of the plots and the frequency of the maximum shifts decreased with increase in temperature. Furthermore, as depicted on the Fig 8, the centre of the arc lies below the real impedance (Z') axis, which suggested non-Debye type dielectric relaxation in BNBTZx samples. This may be due to the presence of distributed elements in the material-electrode system (Macdonald, 1992).

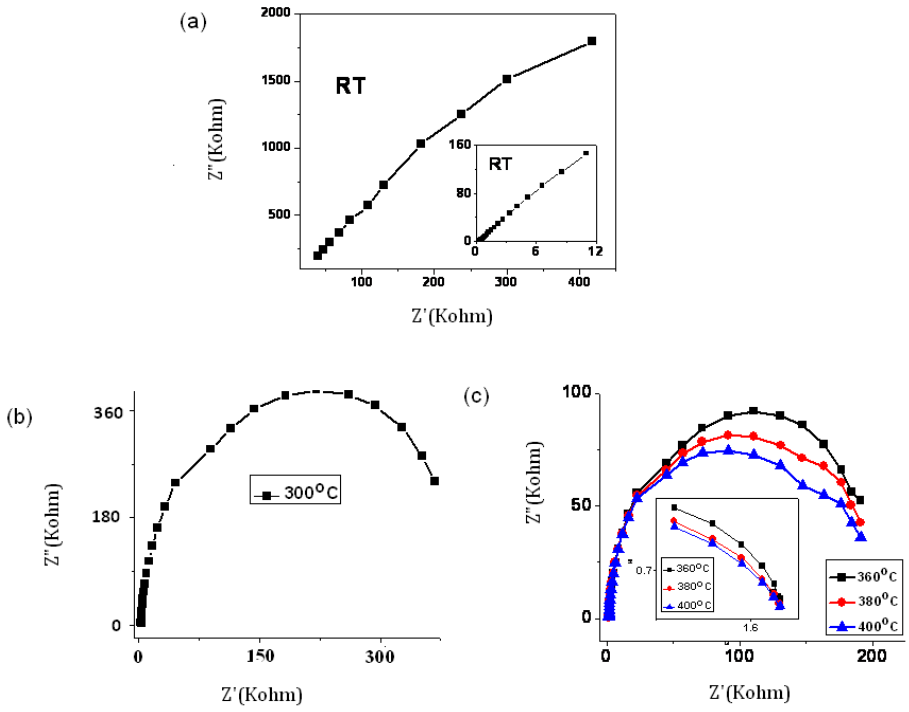

Fig. 8. Cole-Cole plots of BNBTZ4 at various temperatures in kilo scale. The inset in Fig. 8c showed the Cole–Cole plots at and above 360°C which indicates the presence of grain boundary resistance.

3.4.2 A.C and D.C conductivity

The D.C and A.C conductivity behavior in the BNBTZx system has been shown in Fig. 9(a-d). The conductivity of the materials has been found to increase with increase in temperature, and merging of the conductivity curves at higher temperature region results with the release of space charge. The conductivity values at room temperature for BNBTZx of x = 0.0, 0.04, 0.08 and 0.1 are 1.752×10^{-8}(S/cm), 9.348×10^{-8}(S/cm), 8.755×10^{-8}(S/cm) and 6.29×10^{-7}(S/cm) for the respective composition at 1 KHz. It is evident that such conductivity at low temperature is basically due to the migration of ions into vacancies already associated in the compound by thermal energy (Solier et al., 1989). The a.c and d.c activation energies have been calculated from different temperature regions at different frequencies using Arrhenius relation $\sigma = \sigma_o \exp(-Ea/K_BT)$ and the values are given in the Table 2. Where K_B is the Boltzmann constant and Ea is activation energy of the electric conduction. In the low temperature region, the activation energies is in the range of 0.1-0.3eV for BNBTZx system, where x=0.0, 0.04, 0.08 and 0.1 in this region, conductivity is almost independent of temperature and this low value of activation energy corresponds to an intrinsic conduction. The activation energies (0.2-0.4eV) in the second region were slightly increased with an increase in temperature, which suggests that the conductivity may be the result of defects and associated charge carriers of sodium metal ion. In the high temperature region, the activation energies rapidly increased with an increase in temperature to 0.9eV. In high sintering temperature, bismuth ions get evaporated and oxygen vacancies are created for neutralization. These activation energies may correspond to the motion of oxygen vacancies

in the octahedron of the perovskite structure as reported earlier (Warren et al., 1996; Forbess et al., 2000). From the above phenomena it may be deduced that the conductivity at higher temperature region is likely due to motion of oxygen vacancy across the grain-boundary.

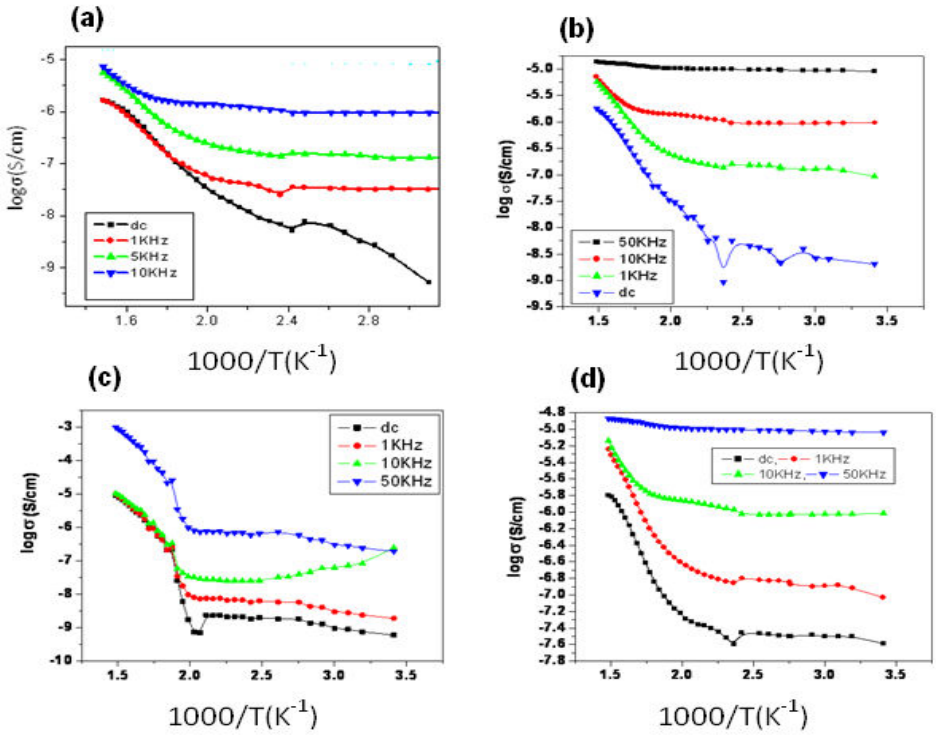

Fig. 9. Plot of A.C and D.C conductivity of BNBTZx samples for x = 0.0, 0.04, 0.08 and 0.10 at 1, 10 and 50 KHz

Table 2. Activation energies of BNBTZx samples for x = 0.0, 0.04, 0.08 and 0.1 in units of electron volts (eV)

Sample composition	Frequency of measurement	Temperature (°C)		
		80-210	230-310	320-400
BNBT	DC	0.125	0.195	0.85
	1KHz	0.205	0.115	0.232
	10KHz	0.141	0.109	0.221
BNBT4	DC	0.11	0.39	0.62
	1KHz	0. 23	0.116	0.93
	10KHz	0.18	0.220	0.800
BNBT8	DC	0.234	0.421	0.393
	1KHz	0.280	0.697	0.727
	10KHz	0212	0.102	0.572
BNBT10	DC	0.231	0.313	0.42
	1KHz	0.11	0.307	0.400
	10KHz	0.19	0.211	0.250

4. CONCLUSIONS

Zirconium substituted Bismuth Sodium Barium Titanate ceramic samples of composition $(Bi_{0.5}Na_{0.5})_{0.94}Ba_{0.06}(Ti_{1-x}Zr_x)O_3$ (for x=0.0, 0.04, 0.08 0.10 and 0.2) were synthesized by solid state method. X-ray diffraction patterns showed formation of phase pure single phase rhombohedral structure for $0.0<x<0.1$. Addition of low Zr^{4+} concentration has no remarkable effect on the crystal structure and grain morphology, the electrical properties of the ceramics are modified. Dielectric studies revealed that the BNBT10 composition exhibit flat curves with low dielectric constant while the other compositions with x=0.0, 0.04 and 0.08 showed broad peaks around the transition temperatures. AC complex impedance studies revealed the existence of grain boundary effect at high temperature, as well as negative temperature coefficient of resistance (NTCR) behavior for the ceramic materials.

ACKNOWLEDGEMENTS

One of the authors (Enyew Amare Zereffa) gratefully acknowledges the financial support from the Government of The Federal Democratic Republic of Ethiopia, through Embassy of the Federal Democratic Republic of Ethiopia, New Delhi (India).

COMPETING INTERESTS

Authors have declared that no competing interests exist.

REFERENCES

Chu, B.J., Chen, D.R., Li, J.R., Yin, Q.R. (2002). Electrical properties of $(Na_{1/2}Bi_{1/2}Ti0_3$-$BaTi0_3$ ceramics. J. Eur. Ceram Soc., 22, 2115 –2121.

Fan, G.F., Lu, W.Z., Wang, X.H., Liang, F. (2007). Effects of manganese additive on piezoelectric properties of $(Bi_{1/2}Na_{1/2})TiO_3$-$BaTiO_3$ ferroelectric ceramics. J. Mater Sci., 42(2), 472-476.

Forbess, M.J., Seraji, S., Wu, Y., Nguyen, C.P., Cao, G.Z. (2000). Dielectric properties of layered perovskite $Sr_{1-x}A_xBi_2Nb_2O_9$ ferroelectrics (A=La, Ca and x=0, 0.1). Appl. Phys. Lett., 76, 2934–2936.

Hegab, N.A., Bekheet, A.E., Afifi, M.A., Wahaba, L.A., Shehata, H.A. (2007). Effect of Cd addition on the A.C. conductivity and dielectric properties of $Ge_{70}Te_{30}$ films. J. Ovonic. Research, 3(4), 71-82.

Herabut, A., Safari, A.J. (1997). Processing and electromechanical properties of $(Bi_{1/2}Na_{1/2})_{(1-1.5x)}La_xTiO_3$. Am. Ceram. Soc., 80(11), 2954-2958.

Kuharuangrong, S., Schulze, W.A. (1996). Characterization of $Bi_{0.5}Na_{0.5}TiO_3$-$PbTiO_3$ dielectric materials. J. Am. Ceram. Soc., 79, 1273–1280.

Lee, J.K., Yi, J.Y., Hong, K.S. (2001). Relationship between structure and dielectric property in $(1-x)(Na_{1/2}Bi_{1/2})TiO_3$ - $xPbZrO_3$ ceramics. Jpn. J. Appl. Phys., Part 1, 40(10), 6003-6009.

Li, H.D., Feng, C.D., Xiang, P.H. (2003). Electrical properties of La^{3+} doped ceramic samples $(Na_{1/2}Bi_{1/2})_{0.94}Ba_{0.06}TiO_3$. Jpn. J. Appl. Phys. Part I., 42(12), 7387-91.

Lu, W., Fan, G., Wang, X., Liang, F. (2007). Phase structure and electrical properties of $Bi_{1/2}Na_{1/2}TiO_3$-$KNbO_3$ lead-free piezoelectric ceramics. Key Eng. Mater., 336(338), 184.

Macdonald, J.R. (1992). Impedance Spectroscopy. Annals of Biomedical Engineering, 20, 289-305.

Nakada, H., Koizumi, N., Takenaka, T. (1999). Lead-free Piezoelectric Ceramics of $(Bi_{1/2}Na_{1/2})TiO_3$– $BiFeO_3$ System. Key Eng. Mater., 169(170), 37–40.

Nagata, H., Takenaka, T. (1997). Lead-free piezoelectric ceramics of $(Bi_{0.5}Na_{0.5})TiO_3$-$0.5(Bi_2O_3$-$Sc_2O_3)$ system. Jpn. J. Appl. Phys., 36(9B), 6055-7

Rao, K.S., Krishna, P.M., Prasad, D.M., Latha, T.S., Hussain, M. (2007). Frequency dependent electrical characteristics of ferroelectric $Pb_{4.0}K_{1.0}Li_{1.0}Nb_{10}O_{30}$ ceramics. Phys. J. Appl. Phys., 239, 237-249.

Sakata, K., Masuda, Y. (1974). Ferroelectric and antiferroelectric properties of $(Na_{1/2}Bi_{1/2})$ TiO_3-$SrTiO_3$ solid-solution ceramics. Ferroelectrics, 7(1-4), 347-349.

Shi, J., Yang, W. (2009). Piezoelectric and dielectric properties of CeO_2-doped $(Bi_{0.5}Na_{0.5})_{0.94}Ba_{0.06}TiO_3$ lead-free ceramics. J. Alloys Compd., 472, 267-270.

Smolenskii, G.A., Isupov, V.A., Agranovskaya, A.I., Krainik, N.N. (1961). New ferroelectrics of complex composition. Sov. Phys. Solid State Engl. Transl., 2, 2651-2654.

Solier, J.D., P´erez-Jubindo, M.A., Dominguez-Rodriguez, A., Heuer, A.H. (1989). Low-temperature ionic conductivity of 9.4-mol%-yttria-stabilized zirconia single crystals. J. Am. Ceram. Soc., 72, 1500-2

Srivaslava, K.K., Kumar, A., Panwar, O.S., Lakshminarayan, K.N. (1979). Dielectric relaxation study of chalcogenide glasses. J. Non-Cryst. Solids, 33, 205-211.

Suchanicz, J., Stopa, G., Kusz, J., Zubko, M., Hofmeister, W., et al. (2010). Structural, thermal expansion and heat capacity study of lead-free $[(1-x)(Na_{0.5}Bi_{0.5})$–$xBa]Zr_1$-$yTiyO_3$ ceramics. J. Mater. Sci., 45, 1453–1458.

Takenaka, T., Maruyama, K., Sakata, K. (1991). $(Bi_{1/2}Na_{1/2})$ TiO_3–$BaTiO_3$ system for leadfree piezoelectrtic ceramic. Jpn. J. Appl. Phys., 30(9B), 2236-2239.

Takenaka, T., Okuda, T., Takegahara, K. (1997). Lead-free piezoelectric ceramics based on $(Bi_{1/2}Na_{1/2})TiO_3$-$NaNbO_3$. Ferroelectrics, 196(1-4), 175-178.

Thongtha, A., Bongkarn, T. (2011). Optimum sintering temperature for fabrication $0.8Bi_{0.5}Na_{0.5}$-$0.2Bi_{0.5}K_{0.5}$ lead-free ceramics by combustion technique. Key Eng. Mater., 474(476), 1754-1759.

Wang, H., Zuo, R., Liu, Y., Fu, J. (2010). Densification behavior, microstructure and electrical properties of sol–gel-derived niobium-doped $(Bi_{0.5}Na_{0.5})_{0.94}Ba_{0.06}TiO_3$ ceramics. J. Mater. Sci., 45, 3677–3682.

Warren, W.L., Vanheusden, K., Dimos, D., Pike, G.E., Tuttle, B.A. (1996). Oxygen vacancy motion in perovskite oxides. J. Am. Ceram. Soc., 79, 536-538.

Wu, L., Xiao, D.Q., Lin, D.M., Zhu, J.U., Yu, P., Li, X. (2007). Temperature dependence of electric properties of $[Bi_{0.5}(Na_{1-x}Ag_x)_{(0.5)}]_{(1-y)}BayTiO_3$ ceramics. Jpn. J. Appl. Phys. Part I., 46(11), 7382-7387.

Xu, C., Lin, D., Kwok, K.W. (2008). Structure, electrical properties and depolarization temperature of $(Bi0.5Na_{0.5})TiO_3$-$BaTiO_3$ lead-free piezoelectric ceramics. Sol. Stat. Sci., 10(7), 934-40

Xu, Q., Chen, M., Chen. W., Liu, H.X., Kim, B.H., Ahn, B.K. (2008). Effect of CoO additive on structure and electrical properties of $(Na_{0.5}Bi_{0.5})_{0.93}Ba_{0.07}TiO_3$ ceramics prepared by the citrate method. Acta Materialia, 56(3), 642-650.